sustainability

MDPI

*Article*

# Social Vulnerability Assessment Using Artificial Neural Network (ANN) Model for Earthquake Hazard in Tabriz City, Iran

**Mohsen Alizadeh [1], Esmaeil Alizadeh [2], Sara Asadollahpour Kotenaee [3], Himan Shahabi [4,*], Amin Beiranvand Pour [5], Mahdi Panahi [6], Baharin Bin Ahmad [7] and Lee Saro [8,9,*]**

1 Department of Urban Regional Planning, Faculty of Built Environment, Universiti Teknologi Malaysia (UTM), Johor 81310, Malaysia; alizadeh.mohsen2003@yahoo.com
2 Faculty of Business and Economic, Technische Universitat Bergakademie Freiberg, 09599 Freiber, Germany; alizadeh.esmaeil.1985@gmail.com
3 Department of Urban Planning, Faculty of Architecture, Civil, Art, Islamic Azad University of Science and Research Branch, Tehran 14778-93855, Iran; asadollahpour.sara@gmail.com
4 Department of Geomorphology, Faculty of Natural Resources, University of Kurdistan, Sanandaj 66177-15175, Iran
5 Korea Polar Research Institute (KOPRI), Songdomirae-ro, Yeonsu-gu, Incheon 21990, Korea; Amin.Beiranvand@kopri.re.kr
6 Young Researchers and Elites Club, North Tehran Branch, Islamic Azad University, Tehran P.O. Box 19585/466, Iran; panahi2012@yahoo.com
7 Department of Geoinformation, Faculty of Geoinformation and Real Estate, Universiti Teknologi Malaysia (UTM), Johor 81310, Malaysia; baharinahmad@utm.my
8 Geological Research Division, Korea Institute of Geoscience & Mineral Resources (KIGAM), Daejeon 34132, Korea
9 Department of Geophysical Exploration, Korea University of Science and Technology, Daejeon 34113, Korea
* Correspondence: h.shahabi@uok.ac.ir (H.S.); leesaro@kigam.re.kr (L.S.); Tel: +98-918-665-8739 (H.S.); +82-42-868-3057 (L.S.)

Received: 25 July 2018; Accepted: 8 September 2018; Published: 21 September 2018


**Abstract:** This study presents the application of an artificial neural network (ANN) and geographic information system (GIS) for estimating the social vulnerability to earthquakes in the Tabriz city, Iran. Thereby, seven indicators were identified and used for earthquake vulnerability mapping, including population density, household density, employed density, unemployed density, and literate people. To obtain more accuracy in our analysis, all of the indicators were entered into a geographic information system (GIS). After the standardization of the data, an artificial neural network (ANN) model was applied for deriving a social vulnerability map (SVM) of different hazard classes for Tabriz city. The results showed that 0.77% of the total area was found to be very highly vulnerable. Very low vulnerability was recorded for 76.31% of the total study area. The comparison of data provided by (SVM) and the residential building vulnerability (RBV) of Tabriz city indicated the validity of the results obtained by ANN processes. Scatter plots are used to plot the data. These scatter plots indicate the existence of a strong positive relationship between the most vulnerable zones (1, 4, and 5) and the least (3, 7, and 9) of the SVM and RBV. The results highlight the importance of using social vulnerability study for defining seismic-risk mitigation policies, emergency management, and territorial planning in order to reduce the impacts of disasters.

**Keywords:** earthquake hazard; social vulnerability map (SVM); artificial neural network (ANN); Tabriz

## 1. Introduction

Earthquake disasters have very strong destructive power, a widespread range, and pose a severe threat to human life safety [1,2]. Iran has one of the highest seismic activity rates in the world, and has experienced many destructive earthquakes in the past. It is one the most vulnerable countries to major earthquake disasters [3]. The Iranian plateau is situated amongst the continental junction of the Arabian and Eurasian plates in the center point of the Alpine–Himalayan seismic belt [4]. According to the earthquakes database, more than 1,000,000 fatalities have been recorded in the past 105 years (since 1900) in Iran, which is one of the worst recorded vulnerability index cases in the world [3,5]. These earthquakes have resulted in the death of thousands of people and the destruction of many villages and cities in the country. For example, the Bam earthquake, which occurred in 2003 (Mw = 6.6) killed over 30,000 people, injured over 10,000, made 100,000 people homeless, and destroyed over 80% of the houses [3]. Based on the statistics of the Iranian plateau, the last century has witnessed 14 major earthquakes of the magnitude of 7 (on the Richter scale) and 51 earthquakes with the magnitude of 6 to 7. However, the earthquakes in Buin-Zahra (1962, Ms = 7.3), Dashte Bayaz (1968, Ms = 7.3), Tabas (1978, Ms = 7.8), Sirch (1981, Ms = 7.3), and Manjil (1990, Ms = 7.7) are other examples [3,6].

It is very difficult to predict earthquakes accurately with the currently available technologies. Vulnerability reduction is a core element of managing or reducing disaster risk, and has been identified as the most significant prerequisite for resilience under degrees of exposure to disasters. Therefore, to reduce the damage caused by earthquake disasters, it is particularly important to study the assessment of social vulnerability to earthquake disasters. Timely and effective disaster risk management strategies not only rely on an adequate understanding of the disaster itself, but should also explore the sense of exposure and vulnerability in the society [7]. The probability of a natural disaster having effects that are more devastating in one place than in another deeply depends on the local vulnerability components of the affected society, such as its sociocultural and economic environment. Indeed, there is an important correlation between the potential risk and the social resistance and resilience of a specific place. Social vulnerability analyses aim to understand which population groups may be the most vulnerable to the impacts of natural hazards and identify the key factors that affect social vulnerability [8]. The results of social vulnerability study can be used in the future for risk management decisions, including risk reduction, prevention, and mitigation [9]. Social vulnerability describes the characteristics of a person or group and their situation that influence their capacity to anticipate, cope with, resist, and recover from the impact of a natural hazard. Socially vulnerable groups are victims who tend to be treated as groups with special needs; these people experience higher social vulnerability, which means that they are more at risk than others are [10].

The concept of social vulnerability within the disaster management context was introduced in the 1970s when researchers recognized that vulnerability also involves socioeconomic factors that affect community resilience [11–14]. Based on the engineering-based paradigm, research on disasters emphasizes the exposure, risk, and assessment of vulnerability to biophysical threats [15–18]. However, over the years, a growing number of studies have opposed this viewpoint, but instead considered disasters as social constructs [19–25]. In the study, the hazards resulting in social vulnerability result in low ability, based on social attributes and contexts, of a group of persons who are exposed to a larger likelihood. For these groups of people, the impact of a disaster presents more difficulties in recuperating from a disaster. The common understanding of vulnerability and its measurability are a means of addressing disasters by setting targets and managing the consequences [26–30]. Due to its complexity, scholars currently have different definitions for the concept of social vulnerability. Koks et al. [31] considered social vulnerability as the ability to deal with disasters. Chen et al. [32] indicated that social vulnerability influences people's ability to make full pre-disaster preparations under the pre-existing conditions, and to recover from post-disaster reconstruction. Clark et al. [33] discussed social vulnerability in reference to the extent of damage caused by a disaster suffered by specific social groups, organizations, or countries [33]. Bankoff et al. [34] noted that vulnerability is the key to understanding risk in attempts to break away from the attitudes that have characterized the

relationships between human societies and their environment. Understanding vulnerability requires more than a simple understanding of societies and their environment; social vulnerability is also about people, their perceptions, and knowledge. However, vulnerability is not a property of social groups or individuals, but rather is embedded in complex social relations and processes. Several other definitions can also be found in the literature. For example, Burton et al. [35] emphasized that social vulnerability is related to all kinds of changes, including natural, social, and individual changes, which expose people to the risk of disaster.

Recently, Rygel et al. [36] developed a method for aggregating vulnerability indicators to obtain a composite social vulnerability index. They identified the indicators of social vulnerability to storm surges associated with hurricanes by reviewing the vulnerability assessment literature. Collins et al. [37] studied the environmental hazards vulnerability in the Ciudad Juarez (Mexico) and El Paso (USA) metropolis. They used the method proposed by Cutter et al. [38] to obtain a social vulnerability index. Wood et al. [39] deciphered community variations in social vulnerability to Cascadia-related tsunamis in the United States (US) Pacific Northwest, by adapting the social vulnerability index (SoVI) at the census-block level [40]. Bjarnadottir et al. [41] developed a coastal community social vulnerability index (CCSVI) for hurricane-prone areas and applied it to Miami-Dade County, Florida, as a case study. Zhang et al. [42] applied a rough set to construct an evaluation model of social vulnerability based on catastrophe progression. Following in-depth literature research, an assessment model of social vulnerability to the earthquake disaster in Sichuan Province, China, based on the catastrophe progression method was established. A rough set attribute reduction method was adopted to eliminate irrelevant social vulnerability indicators and optimize the proposed model. Finally, a catastrophe progression method for social vulnerability to earthquake disaster is developed to overcome the subjectivity of the index weight assignment of social vulnerability indicators in the currently used social vulnerability assessment method. Thiri [43] analyzed the relationship between the environmental migration and social vulnerability of 30 municipalities affected by the 2011 Great East Japan Earthquake Disaster in Miyagi Prefecture. Firstly, the impact of the disaster on migration is estimated using an interrupted time series analysis. Subsequently, migration estimates are regressed using municipality-level data on the impact of the disaster and social vulnerability indicators. In addition, three counterfactuals were created where migration in the absence of the disaster was estimated using different forecasting methods. Cerchiello et al. [44] addressed the assessment of the social vulnerability and resilience level of the city of Nablus, Palestine, which is a region affected by seismic events and political conflicts. The method employed is the scorecard approach (SA), which is a self-assessment and participatory tool that measures resilience with qualitatively derived information at two different urban levels, including population and local administration.

Disaster planning research and management in Iran has focused on the physical aspects of vulnerability and the estimated economic losses due to damaged buildings and infrastructure [3,45–48], thus neglecting the socioeconomic vulnerability component. This study aims to investigate this problem by assessing the social aspect of vulnerability to earthquake hazard using an artificial neural network (ANN). The innovation of this paper addresses three points. First, earthquake disaster occurred frequently in East Azarbaijan Province, but the government and the public's disaster prevention and mitigation response measures were not perfect. Few scholars have chosen to research this region; however, this study chose East Azarbaijan Province as a new research area to provide the basis for disaster risk management departments' decision-making. Second, the determination of the index weights is a difficult problem in the current social vulnerability research literature. The subjectivity of the weighting methods, such as analytic hierarchy process (AHP) or technique for order of preference by similarity to ideal solution (TOPSIS), (AHP) or TOPSIS, has a significant effect on the evaluation results. To solve the problem of weighting, this paper applies the analytical hierarchy process. Third, the ANN-based method here presented meets the requirements demanded for earthquake prediction. This is because current approaches for vulnerability assessment are difficult to implement in a country such as Iran. The computational models derived from artificial neural networks (ANN) [49,50] can

help evaluate earthquake vulnerability despite the inherent and ambiguous nature of earthquakes. The ANN systems can sequentially process information from interconnected units, which reply to inputted variables. These variables include weights, threshold, and transferable mathematical functions. In theory, each unit processes inputs from added units before transferring the signals to another unit in the link. This enhances the capability of the ANN to address complex problems with large data sets and intricate nonlinear relations that comprise numerous diverse alternatives [51]. Furthermore, ANN can recognize complex patterns in data sets that conventional computational procedures are incapable of solving [52,53]. In addition, it delivers consistent predictions, even through uncertain or noisy data [42,54–56]. Consequently, the ANN can effectively generate classified vulnerability maps that originate from complex interactions compared to other classic models, including regression. Moreover, this investigation aims to expose the social vulnerability of Tabriz to an earthquake and discover the statistical findings of a spatial approach. Correspondingly, we wish to introduce a less-known geographical region to broad readerships, and in this way expand the empirical proof of vulnerability assessment. A new research framework was developed to assess the issues of urban social vulnerability by taking Tabriz as a case city and earthquakes as a hazard. This study is helpful in identifying the most and least vulnerable zones in the Tabriz city, and eventually promotes the development of mitigation policies that anticipate the difficulties that accompany urbanization processes and regional demographic shifts.

## 2. Materials and Methods

### *2.1. Study Area*

Tabriz is located in the northwest of Iran (38.08° N, 46.25° E). The city is known as the capital of the province of East Azerbaijan, and is located NW of Iran at 38.08° N and 46.25° E. It consists of nine municipality zones with about 24,559.13 hectares of land area (Figure 1). According to the last census of the Iranian Statistics Center in 2011, Tabriz city has a population of over 1,398,060 [57]. Tabriz county has a population of about 1,579,312 (Tabriz County Governorship, 2011), whereas statistics on the census revealed that the population expanded from 971,482 to 1,545,491 persons at a rate of 1.6 over time. The latest data indicates that Tabriz has experienced significant growth in its population from 1986–2011. Tabriz is the fourth most populated dense city in Iran (besides Tehran, Mashhad, and Esfahan), and serves as a major center for heavy industry and manufacturing. These include industries for automobiles, machine tools, cement production, oil, and petrochemicals. Furthermore, Tabriz has a rich history along with many historical monuments that have been substantially damaged by repeated devastating earthquakes and numerous invasions during the frequent wars [58]. Tabriz city is situated in the vicinity of the North Tabriz Fault (NTF), which is one of the major seismogenic faults [59]. In this region, a large amount of geological and tectonic evidence has been collected to understand the pattern of faulting and its relation to observed seismicity [60]. Earthquake focal mechanisms specify that the WNW trending, right-lateral strike slip comprises many regional faults [61]. Historical records indicate that the previous two large earthquakes that took place on the NTF occurred on adjacent segments 60 years ago around the 18th century [62]. The original earthquake occurred in 1721 with a magnitude of 7.3 on the Richter scale. Starting at 37.90° N, 46.70° E [63], the disaster ruptured along the southeast beside the NTF, stretching over 39 km. The second occurred in 1780 (Ms 7.4), breaking the northwestern section with an epicenter situated at 38.12° N, 46.29° E producing a surface rupture of approximately 100 km in length [63]. Based on the topography of the area under study, the slope decreased marginally from east to west, opening at the basin of Tabriz. The earthquake focal solutions of past earthquakes and global positioning system (GPS) constraints of NW Iran were conducted by Jackson 1992 and McClusky et al. [64]. The results demonstrated that a 22 $\pm$ 2 mm/year convergence exists between the northward shift of the Arabian plate compared to the Eurasian plate, which results in the appearance of many thrusts and strike-slip faults in the region. Based on the probabilistic and

deterministic evaluation, many seismologists predict that a strong earthquake is likely to happen in Tabriz in the coming future [65].

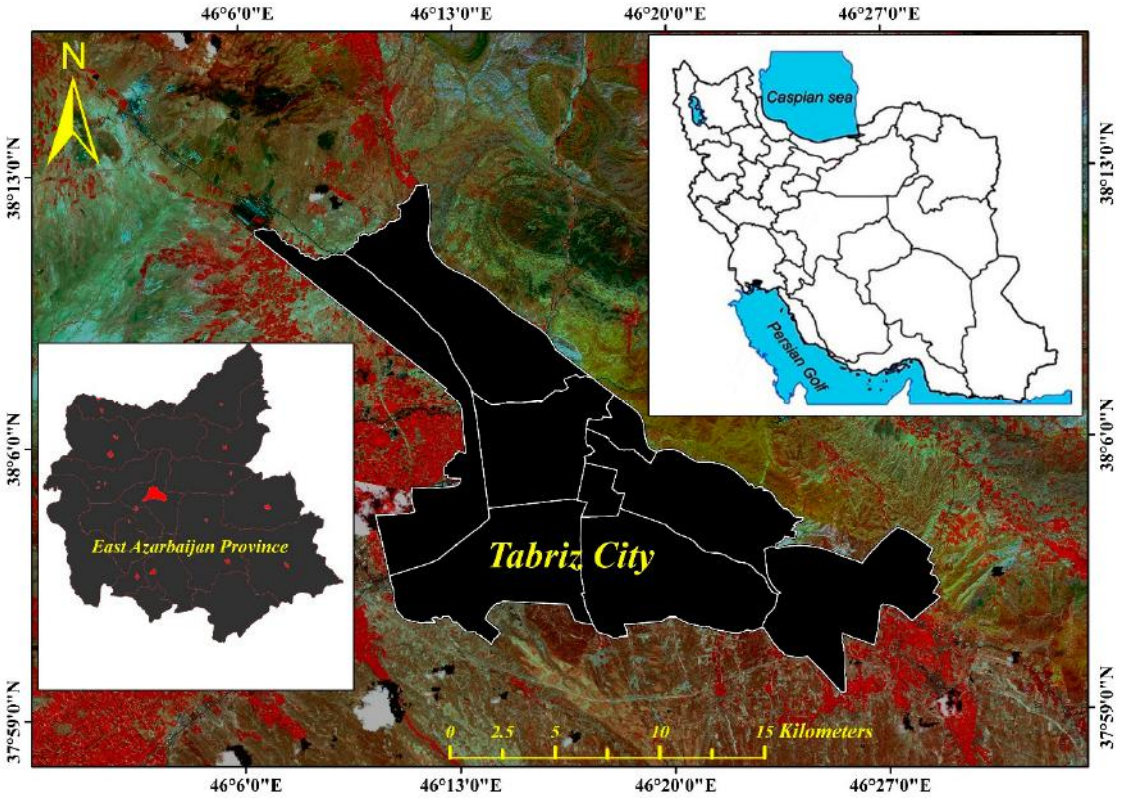


**Figure 1.** General position of Tabriz city and the political provincial and national borders.

*2.2. The Data Sets Used*

Processing of the data for this research was based on the types of data, including data from primary and secondary sources. The primary data were collected using field observations and the distribution of a questionnaire among experts. The sample size is calculated according to the Morgan Table. The use of the sample size determination formula for the 'known' population is not necessary, since the table contains all of the provisions that are required to obtain the requisite size of the sample [66,67]. However, secondary data were collected from different public and private organizations.

The questionnaire was filled out by 10 experts and academics at the geography and urban planning department of the University of Tabriz, and the road and urbanity organization of East Azarbaijan province. The maps of vulnerability can be drafted without accounting for the discrete criteria and indicators that cause heterogeneity in the area of the study. Essentially, this is the most critical aspect of the entire approach; it is required to ensure the adequate selection of the criteria and indicators that account for the complete vulnerability of urban areas in the city of Tabriz. The selection of indicators is an exceedingly laborious aspect of the method, since it comprises the creation of a spatial database for a geographic information system (GIS). Subsequently, the database of GIS enhances serves as input scenarios for earthquake vulnerability analysis during urban earthquakes. Given the objective of this study, the collection of data was performed according to literature-based indicators and a questionnaire surveys from experts.

For this research, a total of 24 social vulnerability (SV) and earthquake hazard indicators for Tabriz city are outlined. Therefore, academics at the geography and urban planning department of the University of Tabriz, along with the road and urbanity organization of East Azarbaijan province, were selected as experts in this study. These specialists were requested to rate the significance of the outlined indicators of vulnerability linked to urban earthquakes in Tabriz, ranging from the

most significant to the least [68]. Consequently, seven indicators were selected and emphasized as indicators related to social vulnerability to earthquakes in the Iranian city of Tabriz. The importance index of specific indicators is subsequently calculated according to the relative importance index (RII) (Equation (1)), which typically range from 0 to 1. The indicators with RII <0.50 were eliminated from the analysis herein.

$$\text{Relative Importance Index (RII)} = \frac{\sum_{i}^{5} Wi}{A \times N} \quad (1)$$

where W is the weight assigned to individual factors by respondents. This can range from one to five, whereas A is the maximal weight (A = 5 in this study), and lastly, N is the number of respondents.

Finally, a total of 17 indicators obtained from the RII with values of <0.50 were acquired, while the remainder was highlighted as nearly or similarly important (RII $\geq$ 0.50). The indicators with <0.5 as earlier mentioned are considered insignificant indicators [69,70]. Therefore, these indicators will not be adopted for analyses. Finally, seven indicators were selected as an input for ANN, including the densities of the population, men, women, literate people, household, employed, and unemployed people. The proposed methodology used in this study is involved in several stages, as illustrated in Figure 2.

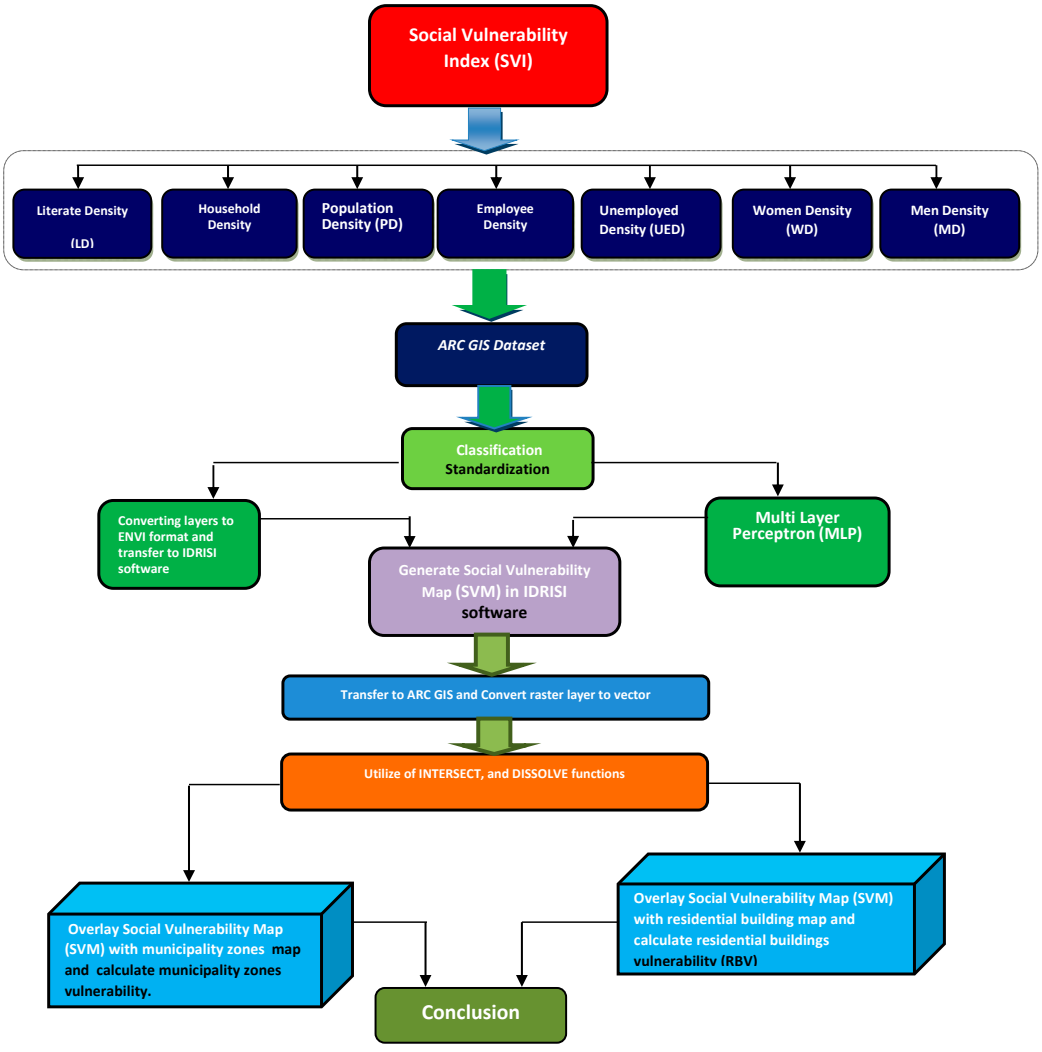


**Figure 2.** Flowchart for proposed methodology used in this study.

### 2.3. Classification and Standardization

Various methods for the mathematical classification of data typically exist in GIS-based software. The methods are constructed on equivalent intervals, manual/natural breaks, or reflections of statistics [71]. In this study, the method of manual classifiers was adopted to recategorize three vulnerability classes based on different values. Therefore, the classification of all of the required layers was initially based on several criteria. These included the density of commercial buildings, learned persons, employed and unemployed individuals, population, and households. Next, all of the layers have been divided into five hazard classes such as very unsuitable, unsuitable, moderate, suitable, and very suitable. The density was subsequently calculated from the kernel density function in the software ARC GIS (version 10.2). The selected radius was 320 with a cell size of 10 (i.e., 10 $\times$10 m). The layer classification was adopted in this phase to define the position of the entire indicators, as it relates to vulnerability zones in various parts of Tabriz. Figure 3 shows the urban social vulnerability indicators produced by GIS in this study. Due to the multiple indicators adopted, each indicator bears a distinct scale value range that necessitates standardization. The process of standardization offers membership significance based on each criterion's utility, as shown in Figure 4 for this analysis.

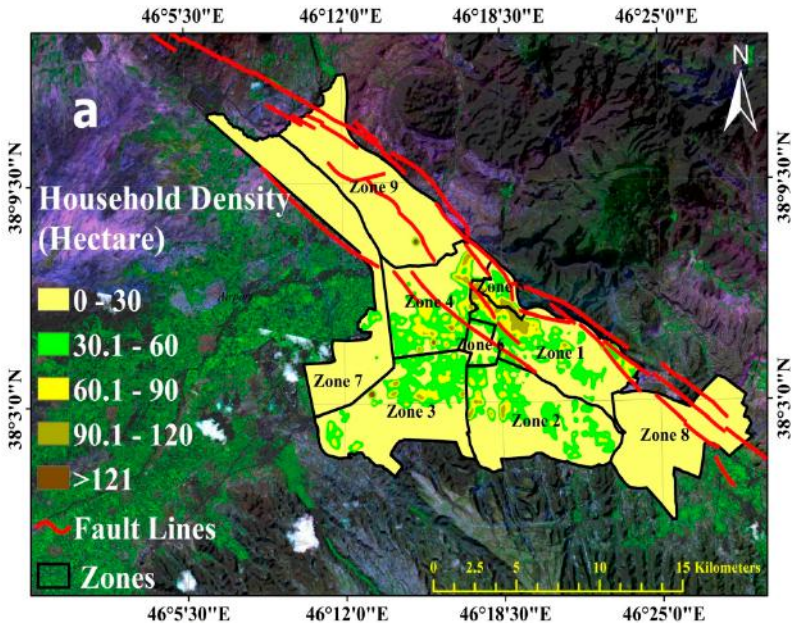


**Figure 3.** *Cont.*

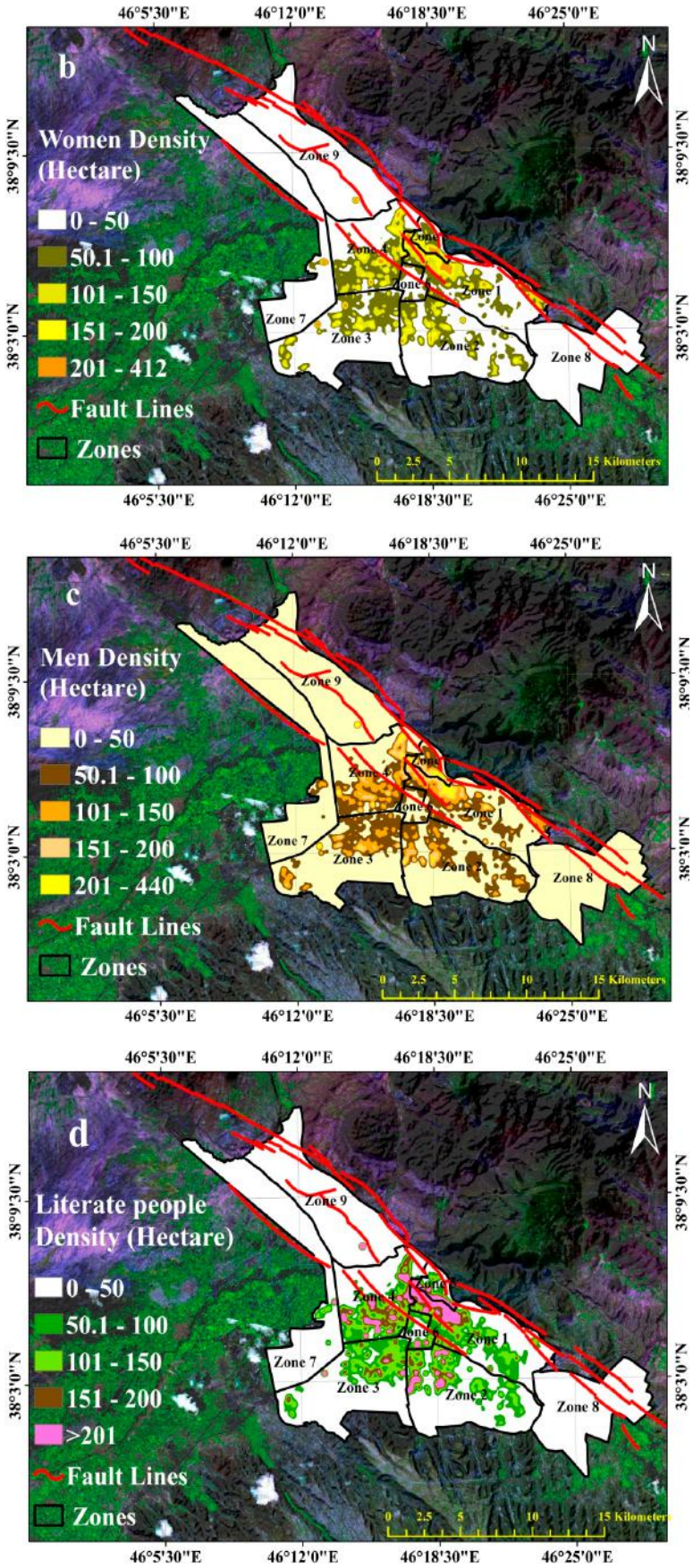


**Figure 3.** *Cont*.

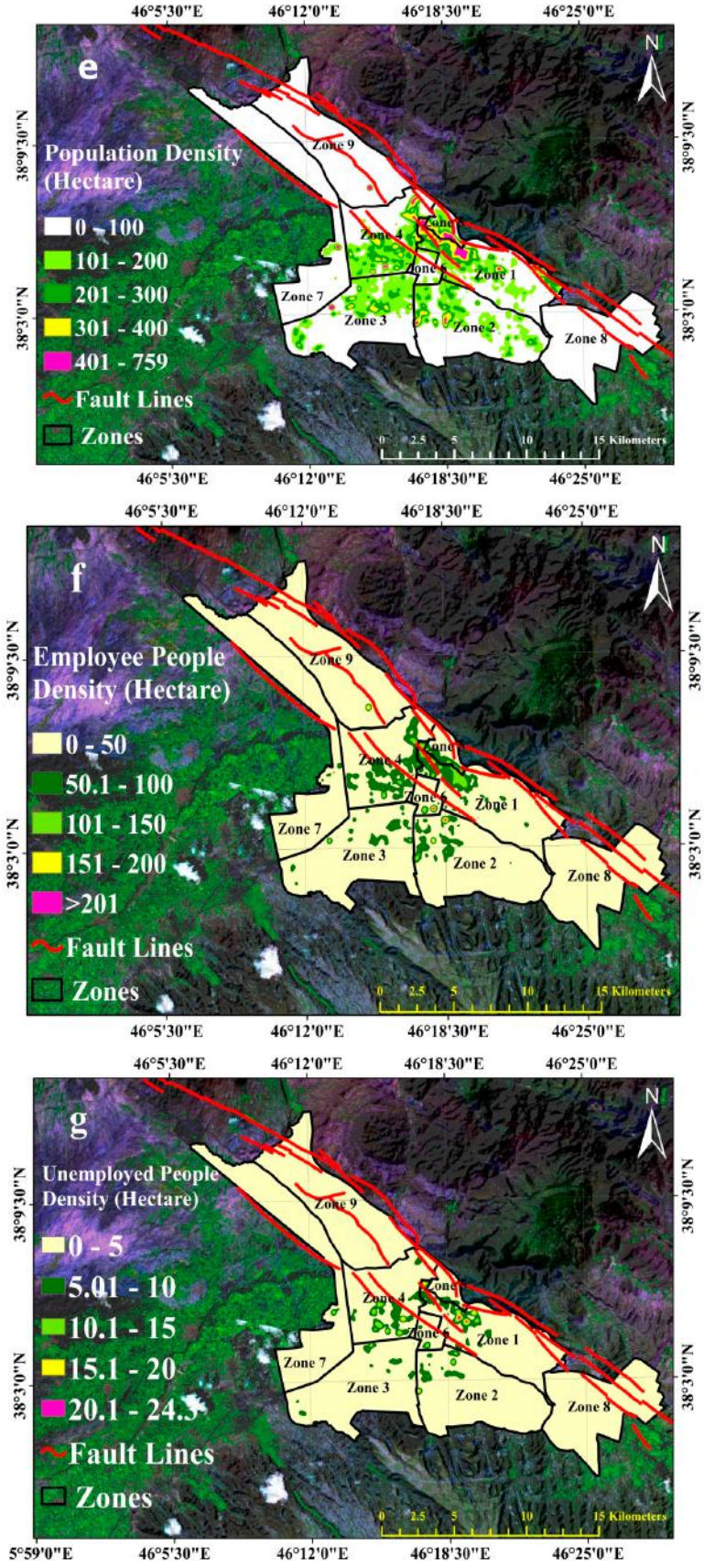


**Figure 3.** Urban social vulnerability indicators produced by a geographic information system (GIS). (**a**) Household; (**b**) Women; (**c**) Men; (**d**) Literate; (**e**) Population; (**f**) Employee; (**g**) Unemployed.

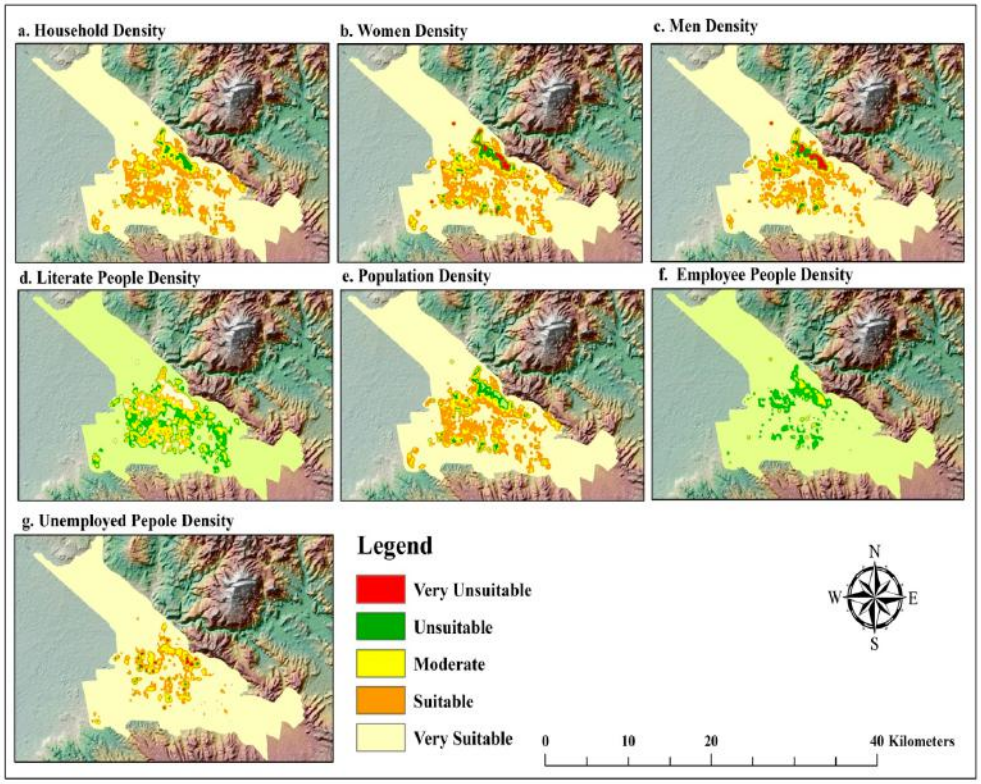


**Figure 4.** Standardization of input layers into with respect to resilience as shown in legend; (**a**) Household Density; (**b**) Women Density; (**c**) Men Density; (**d**) Literate People Density; (**e**) Population Density; (**f**) Employee People Density; (**g**) Unemployed People Density.

### *2.4. Artificial Neural Network (ANN)*

The mathematical models of human perception based on ANNs can be adapted to perform specific tasks based on empirically available data. In the absence of relationships between data, ANN becomes a dominant modeling tool [51,72–76]. The mathematical and theoretical background of ANNs is described in detail by numerous researchers [52,53]. Consequently, only a short explanation is presented hereafter. To sum up, ANN involves layers with a selection of neurons or nodes, which can transform input into output data. Normally, ANN comprises three layers containing input, output, and hidden layers, along with the intermediate areas among them [77]. Among the many aspects that distinguish a neural network from others is its architecture. The architecture presented in this study shows the connectivity patterns among the nodes. This inference is based on the method of defining the connecting weights and activation role [53]. There are two approaches for determining the neural networks architecture: namely, the number of layers (typically single layer, bi-layer, or multi-layer), and the directional flow of information and processing (typically feedforward and recurrent).

The most common ANN is the multi-layer perceptron (MLP) network presented in Figure 5 comprising of three layers, namely input, output, and hidden layers, and the area among them [78]. In this work, the presented algorithms are derived from feedforward multi-layer perceptron (MLP) ANNs that contain distinct layers of hidden neurons amongst the input and output. Hence, the layers of consecutive neurons in MLPs are completely intersected with connection weights that are trainable and control the connections' strength. The training of an ANN is defined by the back-propagation rule of learning. This is an algorithm for iterative gradient descent that is designed to diminish the mean square error between the desired vectors for the target and actual output. It noteworthy to state that the method of gradient descent occasionally experiences slow convergence. This is typically attributed to the presence of various local minima that may also influence the final training results. Such problems are addressed by repeated training by reorganizing the preliminary conditions and the verification

of each training process that resulted in similar convergent findings in terms of the R2 and RMSE. This can be accomplished by increasing the variables until the improvements that are obtained are negligible. The optimal architecture of ANN is described based on the total neurons and hidden layers. However, the best strategy begins with an easy architecture for ANN, typically with a single layer of limited hidden neurons. The ANN was trained by a subclass of data available for testing, whereas the remaining data set was compared with the training and testing errors. Next, the ANN structure is enlarged by the addition of neurons and hidden layers. The training and testing are subsequently repeated, and errors are recomputed until further changes with a negligible decrease of the training error and an increase in the test error in the ANN architecture are obtained. This procedure permits the definition of the minimal ANN architecture that is suitable for providing an adequate fit for the training data that can avert problems with overfitting. The concept of overfitting is associated with the oversizing of the ANN, which causes substantial errors when the input data for testing the ANN is not part of the set for training [79,80]. However, the ANN can accurately replicate the training, although it typically fails the procedural test [81].

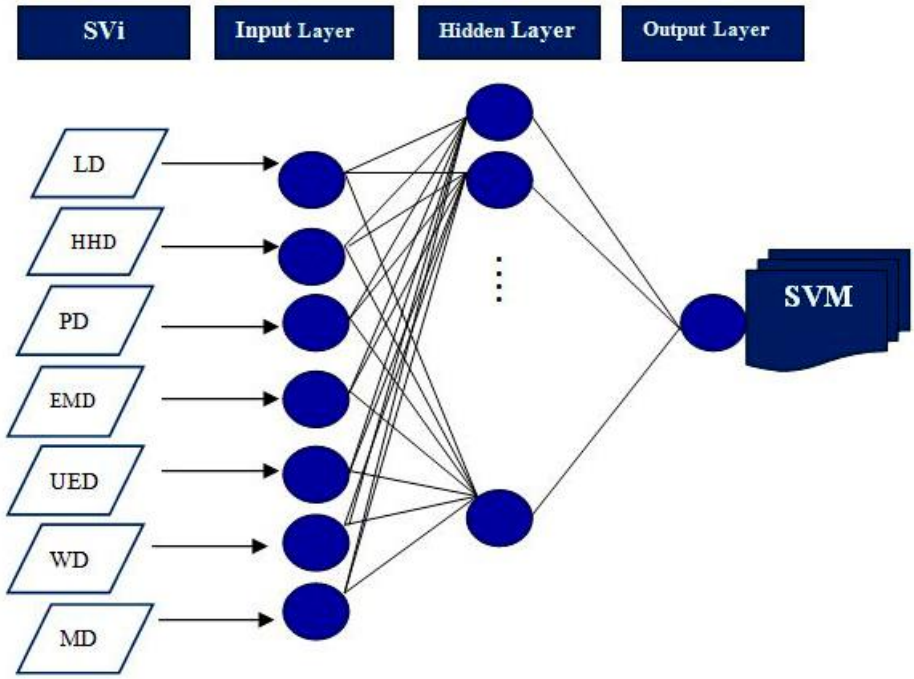


**Figure 5.** The architecture of a multi-layered artificial neural network (ANN) used in this study.

The data is received from the input layer located at different locations such as the thematic layers. Thus, the layers of input neurons require a number of input sources of data. Therefore, the actively processed data exists in the hidden and output layers. However, the number of hidden layers and its neurons is determined by trial and error [82,83]. The number of neurons in the output layers is determined by the application, which for this study is represented by the mapped class. The hidden neuron of each responds to the weighted inputs it receives from the connected neurons at the previous input layer [56]. When the weighted input sums to every hidden neuron are determined, the neuron's activation is specified through the transfer functionality. As a result, the signal flow from the input is termed $x_1$ to $x_n$, which is assumed to be unidirectional as revealed by arrows, which signify the output signal flow (*0*) of the neuron. Therefore, the output signal *0* of the neuron is represented by the relationship:

$$0 = f(net) = f\left(\sum_{j=1}^{n} w_j x_j\right) \quad (2)$$

where $W_j$ are the weight vector, and the function $f(net)$ is referred to as an activation (transfer) function? The variable *netis* is defined as a scalar *net* product of the weight and input vectors:

$$net = w^T x = w_1 x_1 + \ldots + w_n x_n \tag{3}$$

where $T$ is the transpose of a matrix, and, in the simplest case, the output value 0 is computed as:

$$0 = f(net) = \begin{cases} 1 \text{ if } w^T x \geq \theta \\ 0 \text{ otherwise} \end{cases} \tag{4}$$

where $\theta$ is called the threshold level, and this type of node is called a linear threshold unit [84].

### 2.5. Data Analysis

The social vulnerability (SV) to the hazards of earthquakes in Tabriz city was assessed using the multi-layer perceptron (MLP). The MLP was operated in the mode for hard classification using the software IDRISI software (version 17.1, Clark University, Worcester, MA, USA). Next, the opening indicator weights were randomly selected to begin the process of training. The data for the raster training sites were classified as byte or integer category-type files. The process of training decreases the errors in the output and real data of the ANN by modifying the weight-based algorithm [76]. For every category in the files for site training, the numerical pixels for each class were randomly allocated between the training and testing routines. In addition, the total pixels adopted are specified by the ratio among the specified numbers of the maximal training and testing pixels. Based on the similar values for every entry, the pixels are divided at a ratio of 1:1. On the whole, the range is from hundreds to thousands, as opposed to the high number of pixels per category.

For this study, 700 pixels in each class on average for training and testing in the city of Tabriz (see Table 1) was selected. The results of the analysis and testing pixels were validated using the training pixels. The topology of the network was comprised of 10 nodes per each hidden layer, with five layers each of input and output nodes. The total layers of input were identified by a number of images, whereas the layers of output were by the categories of the training site in the file for training. The following steps account for the parameters for training in which the crucial aspect involves the learning rate. Typically, this is a positive constant, which controls the modification performed on the connecting weights. Therefore, automatic training and the dynamic rate of learning were utilized. In theory, automatic training amends the rate of learning during the training process. The use of dynamic learning requires input for the start-learning and end-learning rates. Hence, the inputted learning rate and momentum factor are 0.01 and 0.5, correspondingly. When the learning rate is minimized, the time in the training phase increases; however, a large rate of training results in poor results characterized by inconsistent adjustments. In this study, the momentum factor was adopted to promote the procedure for convergence. Typically, the criteria to terminate the procedure is ensured by making the necessary adjustments. Lastly, the measurement of the acceptable error from the RMS (root mean square) related to network learning:

$$\text{RMS} = \frac{\sqrt{\sum_p \sum_k (t_{pk} - o_{pk})^2}}{P \times N} \tag{5}$$

The RMS determined in this study was 0.1168, and is adequate with respect to the IDRISI default of 0.5. However, if the acceptable error is very small, it will be challenging for the results to converge. Therefore, additional iterations could result in over-training. The training procedure was subsequently terminated at the specified iterations of 15,000. Lastly, the rate of accuracy was according to the characteristics of the sampling training and categorized testing pixels.

**Table 1.** Network, data, and training parameters used for multi-layer perceptron (MLP) for vulnerability map in IDRISI Selva software. RMS: root mean square.

| Group | Parameter | Value |
|---|---|---|
| Input specifications | Avrg. training pixels per class | 700 |
| | Avrg. testing pixels per class | 700 |
| Network topology | Hidden Layers | 1 |
| | Nodes | 10 |
| | Input Layers Node | 5 |
| | Output Layer Nodes | 5 |
| Training parameter | Automatic training | Yes |
| | Dynamic learning rate | Yes |
| | Start Learning rate | 0.001 |
| | End learning rate | 0.0001 |
| | Momentum factor | 0.5 |
| Stopping criteria | RMS | 0.1168 |
| | Iterations | 15,000 |
| | Accuracy rate | 95.66 |

Based on this analysis, the overall accuracy of 95.66% was recorded for the testing data using an ANN. This specified rate was according to the characteristics of the sample training and testing pixels for the category. The last stage of ANN analysis was the drafting of the social vulnerability map (SVM) and earthquake vulnerability map. To accomplish this, the trained and tested architecture for ANN was subjected to the derivative sets of data to produce the SVM of the area under study. After the SVM was produced, the map was imported into the GIS environment. Next, the raster map was adapted into the vector format whilst processing the Dissolve function required to compute the city's vulnerability based on the area per hectare (Table 2).

**Table 2.** Level of vulnerability in Tabriz city.

| Vulnerability | Hectare | Area ($m^2$) | Percent |
|---|---|---|---|
| Very High | 196.01 | 1,960,132.47 | 0.77 |
| High | 541.27 | 5,412,691.087 | 2.11 |
| Moderate | 1036.01 | 10,360,052.8 | 4.04 |
| Low | 4295.37 | 42,953,682.7 | 16.77 |
| Very Low | 19,550.56 | 195,505,633.7 | 76.31 |
| SUM | 25,619.22 | 256,192,192.8 | 100 |

## 3. Results

This study has been concerned exclusively with the construction of a set of composite indicators for social vulnerability assessment (SVA) in the context of earthquake hazards, which was proposed and implemented on real data of statistical units of municipality zones in Tabriz city. After computing the scores for the seven social indicators, the next step is first visualizing the obtained results for a better understanding of earthquake vulnerability for the nine municipality zones in Tabriz, and then validating the results. The constructed composite indicators in this study are expressed via the ArcGIS software. Visualization of the results represents a better understanding of the variation of the resilience level. The results clearly illustrate the difference between the north and south of the city.

Results indicate that Tabriz city is largely categorized into five (5) vulnerable zones. These include very high, high, moderate, low and very low, which are based on the seismic hazards related to the future occurrence of earthquakes. It is noteworthy to state that the five (5) categories were applied to highlight that specific regions are more vulnerable than others. After computing the scores for the social vulnerability index and the five (5) indicators for social vulnerability, the synthetic social vulnerability scores were subsequently displayed as a five-category map through ArcGIS (10.3).

As shown in Table 2, the differences in the vulnerability levels are observable within the study area. The findings demonstrate that of the total area, 0.77% can be described as highly vulnerable. Therefore, the vulnerable zones that are described as high, moderate, and low signify 2.11%, 4.04%, and 16.77% of the area, respectively. The low vulnerability study area accounted for 76.31% of the total. Taking into account the municipal zones map and SVM of Tabriz, the vulnerability levels of the numerous zones are presented in Figure 6. However, selected regions of Tabriz are located in the moderate-to-high hazard seismically zones. For nine zones in Tabriz, the seismic vulnerability reveals that many zones in the city are situated in a low to medium threshold of damage.

However, the south and southeast regions of the city are in suitable condition based on vulnerability. Given this, the zones such as 5, 4, and 1 are considered highly damaged areas. The maximal seismic vulnerability was observed in zone 5 due to its higher density of buildings in an area classified as one of the oldest in the city of Tabriz. The highest population among the nine zones in the city is zone 5, which has high probabilities of human casualties from potential earthquakes in this area. Other extremely populated areas are zone 4 and 1. Moreover, the highest buildings density in Tabriz can be found in zones 5, 4 and 1. Based on the data provided by SVM, zone 5 is classified in the very high and high vulnerability categories based on the values of 21.77% and 22.39%, respectively. As stated, the second most vulnerable area is zone 4, with 0.93% and 41.69%, which is categorized as very high and high vulnerability, respectively. Lastly, the third most precarious zone in Tabriz is zone 1, with 9.68% and 15.60%, which is categorized as very high and high vulnerability (see Figure 6, Table 3).

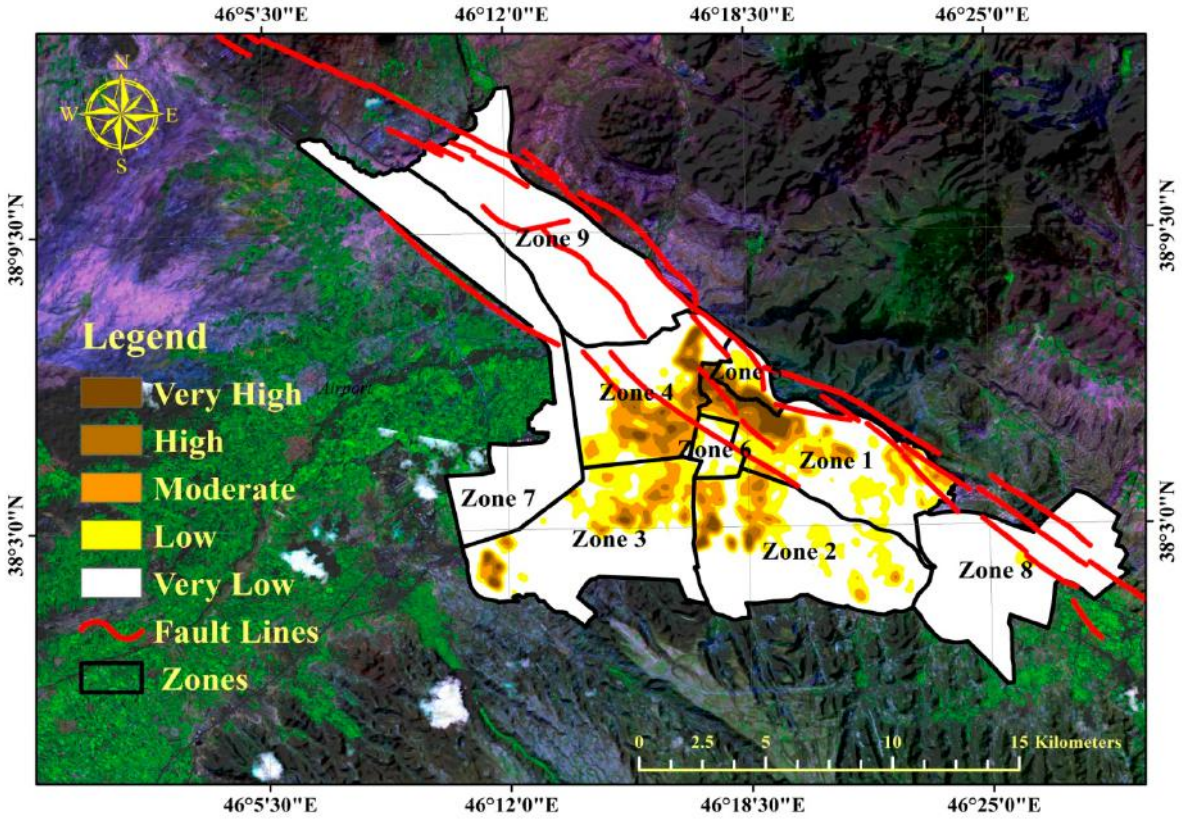


**Figure 6.** Social vulnerability map (SVM) extracted from the proposed model.

**Table 3.** Level of the vulnerability of municipality zones according to the proposed model.

| Vulnerability | Very High | High | Moderate | Low | Very Low | Percent |
|---|---|---|---|---|---|---|
| Zone 1 | 9.68 | 15.60 | 7.66 | 24.66 | 42.39 | 100.00 |
| Zone 2 | 0.35 | 1.74 | 5.38 | 28.05 | 64.49 | 100.00 |
| Zone 3 | 0.25 | 1.49 | 4.96 | 27.56 | 65.73 | 100.00 |
| Zone 4 | 0.93 | 41.69 | 12.93 | 25.21 | 19.23 | 100.00 |
| Zone 5 | 21.77 | 22.39 | 8.47 | 25.34 | 22.04 | 100.00 |
| Zone 6 | 0.00 | 0.00 | 1.10 | 30.75 | 68.15 | 100.00 |
| Zone 7 | 0.00 | 0.24 | 0.02 | 1.72 | 98.02 | 100.00 |
| Zone 8 | 0.00 | 0.00 | 0.00 | 0.00 | 100 | 100.00 |
| Zone 9 | 0.23 | 0.05 | 0.10 | 99.5 | 0.13 | 100.00 |

Conversely, the high social vulnerability score for these zones are based on different factors. To begin with, the higher population density in zone 5 exposes people to earthquakes. Consequently, the casualties, losses, and social vulnerability to earthquakes is significantly higher. Secondly, the level of regional economic development determines the quality of public infrastructure. Therefore, higher regional economic development ensures the availability of community service facilities, which includes better disaster response and recoverability. The public infrastructure in zone 5 is at a lower level than other zones, which means its social vulnerability to earthquakes is comparatively higher. Furthermore, the critical areas of zones 5, 4, and 1 are responsible for the vulnerability of some areas of Tabriz city, particularly at locations near the North Tabriz Fault (NTF). On the other hand, zone 8 with 100% very low vulnerability categories, shows the lowest vulnerability. Then, zone 7, with 1.72% and 98.02% in the low and very low vulnerability categories, is the second least vulnerable zone among the zones. Thereafter, zone 9 with 99.5% and 0.13% in low and very low vulnerability categories is classified as the third least vulnerable zone.

The social vulnerability in the selected zones is low due to the rebuilding efforts of the community and government. The use of high-quality building materials, robust designs, and the construction of houses with fewer levels has been implemented. In addition, the provision of generous subsidies and employment opportunities for victims by the government has prominently improved income levels. It stands to reason that higher per capita incomes result in wealth accumulation by families, and by extension stronger access to community resources. Lastly, the increased access to health-care services and facilities was increased by the government.

However, it is obvious that the northern regions of the city have a relatively better situation. This study estimated the southern parts of the city are faced with the highest earthquake risk. According to their final report, regions 5, 4, and 1 were defined as the most dangerous areas, which are so close to the North Tabriz Fault (NTF) and will experience the high seismic intensity and population damages. In fact, the spatial outcome of the SVM shows that such administrative subdivision in Tabriz can help better understand and synthesize the general characteristics of the city in relation to social vulnerability, and which of the systems have a major role in the different areas of the city. These results point to the heterogeneous spatiality distribution of SV, which affects the overall vulnerability of the city in different ways and with different intensities. This suggests the need to intervene in all of the systems to enhance the overall city's resilience. On the other hand, interventions in Circumscription 1, which presents a higher SVA, can be considered as a priority in order to reduce the social vulnerability to earthquakes in Tabriz.

## 4. Discussion

The concept of social vulnerability stimulates people to make forehand preparations against disasters. These arrangements made during pre-existing conditions can enhance the capacity for communities to recuperate during the period of post-disaster reconstruction. As such, the concept is a social construct that exposes the stratification and disparity between different people, groups, or places. Therefore, the reduction of social vulnerability necessitates considerations for the

fundamental features of the socioeconomic and local terrain. However, there is a lack of consistent metrics for evaluating social vulnerability to earthquakes. Currently, the indicators of social vulnerability are developed from statistical data. Therefore, the data that is available significantly influences the selection of indicators, which is a process that depends on readily quantifiable variables, although these might not be accurate for assessing social vulnerability. Cutter et al. (2003) [40] created social vulnerability indicators that are described in a statistical yearbook published in the United States.

In Iran, as a developing country, a social vulnerability can play a greater role in the overall vulnerability to natural hazards than elsewhere [85–88]. Consequently, in order to reduce vulnerability, risk-reduction strategies must consider as much as possible the population's characteristics and ensure that the population knows how to act in emergency situations. Similarly, institutions must have a clear picture of what preventive measures can be employed, both at the individual and the community level, to reduce the risk for individuals, households, and communities. As it has been observed, supporting the local community's involvement is crucial for implementing strategies that will lead to a culture of safety [89]. However, Iranian researchers have examined the concept based on various yearbooks available in Iran. Consequently, there is a significant difference between foreign and domestic scholars in the construction of indicators that describe social vulnerability. Furthermore, based on the disparities in political and cultural backgrounds, ethnic factors need to be considered by foreign scholars during the development of social vulnerability indicators, although Iranian academics do not take these factors into cognizance. The vulnerability of Iran to earthquakes is influenced by multi-dimensional factors classified as socioeconomic, physical, and environmental. In this paper, socioeconomic factors are considered the key element that influences earthquake vulnerability studies in Iran.

Tabriz city is located among a number of seismic faults with the high potential of earthquake occurrence. Its residential areas are highly vulnerable to earthquakes due to dense population, too many structures, and violations of construction codes [64,65]. Thus, in the case of an earthquake, the possibility of a severe damage will increase dramatically. Therefore, developing a seismic vulnerability map is a useful step to take in order to decrease the severity of a major earthquake impact in the area. The construction of vital structures such as hospitals and schools can be limited in highly vulnerable areas, and the establishment of vital roads can be banned or subject to observing all of the earthquake engineering principles, seismic regulations, and construction codes. The elaboration of SVA and SVM helped identify social vulnerability and visualize how it spreads spatially in Tabriz city. However, the data on the size and area of the vulnerable zones alone cannot highlight the probable impact or risk levels. Hence, data on residential buildings in the municipality zones of Tabriz can be adapted to estimate or forecast the vulnerability impact of Tabriz. Therefore, the residential building vulnerability (RBV) in different zones of Tabriz is deduced as depicted in Figure 7.

Comparing the SVM with data provided by residential buildings may enable researchers to analyze the amount of vulnerability more accurately. Table 4 compares the vulnerability zones outlined for Tabriz city as derived from the SVM and residential building vulnerability (RBV) data. As observed, the most exposed zones are collected in zones 5, 4, and 1 of the city. These three zones due to their location on the North Tabriz Fault (NTF) specified as most vulnerable zones.

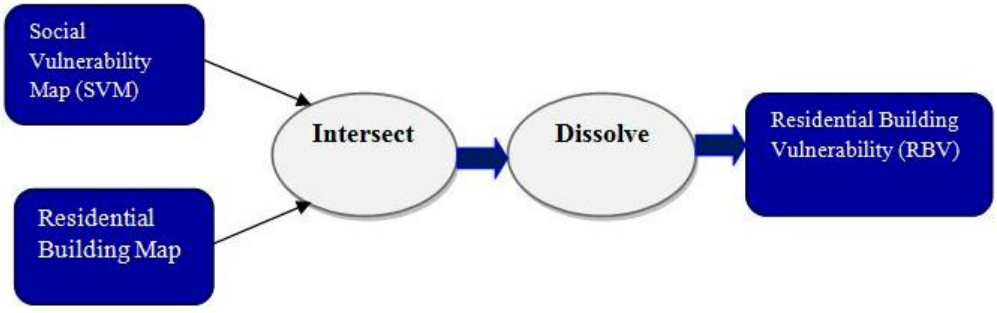


**Figure 7.** The procedure of determining population vulnerability.

By overlapping the SVM and residential buildings vulnerability (RBV), it is possible to see that the lowest vulnerability zones are zones 3, 7, and 9. In this study, the urban vulnerability of Tabriz city against earthquake hazard has been investigated according to social indicators using the artificial neural network (ANN) model. The planned framework for vulnerability assessment is a flexible application for urban environments at various geographical scales and mapping units. However, limitations exist for applying social vulnerability indicators in the city of Tabriz. The key difficulty is a lack of data quality. Nevertheless, this paper has adopted suitable variables to explain most of the social vulnerability changes in the city of Tabriz. The data adopted for this study includes the current population census from 2011. This availed the authors with the most up-to-date information for the comprehensive understanding of the high spatial and social vulnerability distribution in the city. The results showed that that high disparities in social vulnerability to the hazards of earthquakes are prominent in the city of Tabriz. This is because all of the management strategies for earthquake hazards are based on a biophysical component of place vulnerability [90]; this calls for a serious reconsideration of these strategies and the incorporation of a social vulnerability component in these strategies.

**Table 4.** Level of residential building vulnerability (RBV) according to the proposed model.

| Vulnerability | Very High | High | Moderate | Low | Very Low | Percent |
|---|---|---|---|---|---|---|
| Zone 1 | 12.53 | 16.42 | 32.03 | 37.06 | 1.95 | 100.00 |
| Zone 2 | 0.68 | 29.45 | 38.71 | 27.99 | 3.17 | 100.00 |
| Zone 3 | 0.00 | 10.81 | 5.44 | 31.67 | 52.08 | 100.00 |
| Zone 4 | 3.19 | 52.68 | 31.80 | 11.51 | 0.82 | 100.00 |
| Zone 5 | 33.50 | 25.53 | 26.76 | 14.20 | 0.01 | 100.00 |
| Zone 6 | 0.00 | 16.11 | 53.42 | 28.85 | 1.62 | 100.00 |
| Zone 7 | 0.00 | 0.00 | 3.68 | 4.36 | 91.95 | 100.00 |
| Zone 8 | 0.00 | 0.00 | 54.4 | 44.9 | 0.6 | 100.00 |
| Zone 9 | 0.00 | 0.00 | 20.78 | 79.23 | 0.00 | 100.00 |

## 5. Investigating the Accuracy of the Obtained Results

The last step toward constructing composite indicators is the validation and verification of the model. Validation is a set of methods for judging a model's accuracy in making relevant predictions [75]. In this study, standardization of data has divided it into five classes of very suitable, suitable, rather suitable, unsuitable and very unsuitable, with values of 5, 4, 3, 2 and 1, respectively. Hence, the domain of interest that adequately and accurately represents the constructed model was developed. It is noteworthy to state that there is the likelihood that the required accuracy might not be accomplished through the standardized or classified data presented in this paper. Nevertheless, it is desirable that the domain stated is developed in the model's output, since it signifies the model's flexibility and compatibility from the human standpoint, as verified in this study. As a result, the results of the SVM were compared to RBV to validate the findings of our proposed model. The results from both methods are presented in the form of the scatter plots presented in Figures 8 and 9. The scatter plots specify a strong positive connection between the most vulnerable zones (1, 4, and 5) along with the least vulnerable zones (3, 7, and 9) based on the SVM and RBV. Additionally, Spearman correlation coefficients between the most and least vulnerable zones of the two mentioned outputs were calculated (Tables 5 and 6). The coefficient of correlations was 0.997 and 0.921 (statistically significant at 0.01 and 0.05 levels) between the most and least vulnerable zones, respectively. The findings show that the outputs are in agreement based on the vulnerability levels examined in the zones.

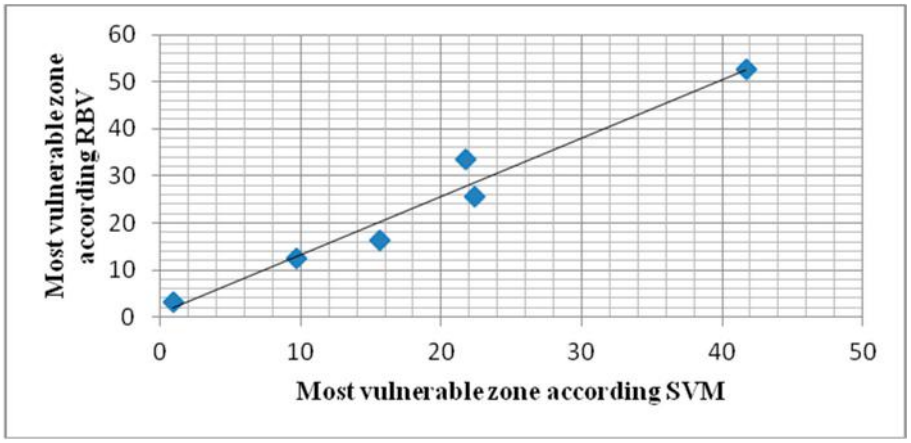


**Figure 8.** The scatter plot between the SVM and RBV according to the most vulnerable zones.

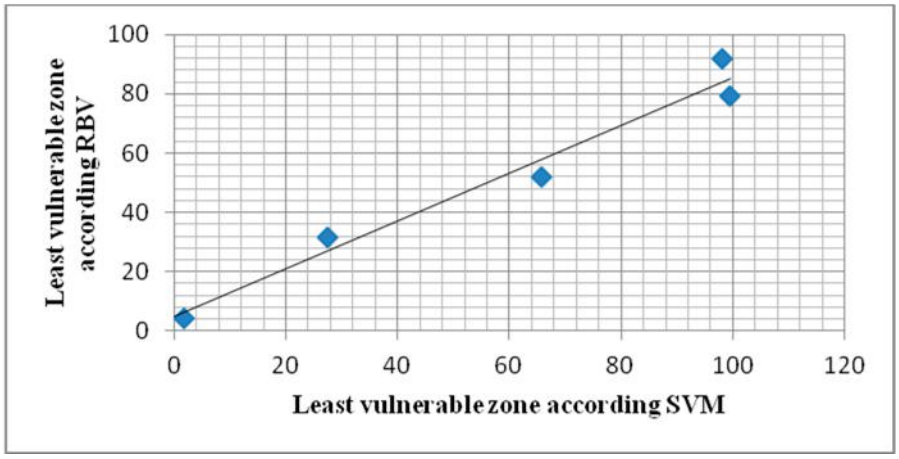


**Figure 9.** The scatter plot between the SVM and RBV according to the least vulnerable zones.

**Table 5.** Correlation between the SVM and RBV for the most vulnerable zones.

| | | SVM | RBV |
|---|---|---|---|
| SVM | Pearson Correlation | 1 | 0.997 ** |
| | Sig. (2-tailed) | | 0.000 |
| | N | 6 | 6 |
| RBV | Pearson Correlation | 0.997 ** | 1 |
| | Sig. (2-tailed) | 0.000 | |
| | N | 6 | 6 |

** Correlation is significant at the 0.01 level (two-tailed).

**Table 6.** Correlation between the SVM and RBV for the least vulnerable zones.

| | | SVM | RBV |
|---|---|---|---|
| SVM | Pearson Correlation | 1 | 0.921 * |
| | Sig. (2-tailed) | | 0.026 |
| | N | 5 | 5 |
| RBV | Pearson Correlation | 0.921 * | 1 |
| | Sig. (2-tailed) | 0.026 | |
| | N | 5 | 6 |

* Correlation is significant at the 0.05 level (two-tailed).

## 6. Conclusions

The objective of this research is to assess the social aspects of vulnerability for earthquake hazard and apply it at a municipality level in Tabriz city, northwestern Iran. In order to assess urban vulnerability to earthquake hazard, this research developed a novel computational framework to assess the social dimension of vulnerability. This investigation contributes to (i) the significance of indicators of social vulnerability, which are typically deduced from the relative importance index (RII); (ii) the correlation between the input and output data set variables, which is nonlinear, were detected through the ANN (artificial neural network) model. The proposed model adopted the process of learning (training) to appraise the output and input data variables; and (iii) the confirmation of the model demonstrated a strong positive relationship between the most vulnerable and least vulnerable zones based on the evaluation of the SVM and RBV. Therefore, a novel perspective was selected, and the application of ANN to an actual world case study shows that the new technique is robust for evaluating social vulnerability. Furthermore, social vulnerability mapping delivers an avenue to transport specific information about the most vulnerable areas to the effects of earthquakes. The findings also denote a vivid existence of spatial clustering between the low and highly vulnerable social groups. In the case, the northwest district is classified as very highly socially vulnerable for example in zone 5, whereas the north and eastern regions such as zone 7 are low. Consequently, the evaluation of social vulnerability can assist in developing strategies that are crucial to localities and improve understanding of the patterns of vulnerability in these regions. In the long term, this will ultimately assist in the formulation of mitigation policies that can anticipate the problems associated with the processes of urbanization and demographic shifts in the regions examined. Policy makers, decision makers, and urban planners can apply the resultant data provided by SVM and RBV to reduce the damage and human causalities and reduce the losses that might be caused in future earthquakes by means of mitigation prevention and avoidance.

**Author Contributions:** M.A., E.A. and S.A.K. collected field data and conducted the earthquake hazard and analysis. H.S., A.B.P., M.P., B.B.A. and L.S. are contributed to the work especially in re-constructing and editing the revised manuscript. B.B.A. and L.S. contributed in funding acquisition too.

**Funding:** This research was supported by the Basic Research Project of the Korea Institute of Geoscience, Mineral Resources (KIGAM) funded by the Minister of Science and ICT and Universiti Teknologi Malaysia (UTM) based on Research University Grant (Q.J130000.2527.17H84).

**Acknowledgments:** We are thankful to Korea Polar Research Institute (KOPRI) for cooperation during producing of the primary version of the manuscript.

**Conflicts of Interest:** The authors declare no conflicts of interest.

## References

1. Xu, C.; Dai, F.C.; Xu, X.W. Wenchuan earthquake-induced landslides: An overview. *Geol. Rev.* **2010**, *56*, 860–874.
2. Zhang, J.S.; Jia, Z.K. The study on assessment index of urban social vulnerability to the earthquake disaster. *Technol. Guide* **2010**, *36*, 12–14.
3. Zebardast, E. Constructing a social vulnerability index to earthquake hazards using a hybrid factor analysis and analytic network process (F'ANP) model. *Nat. Hazards* **2013**, *65*, 1331–1359. [CrossRef]
4. Panahi, M.; Rezaie, F.; Meshkani, A.S. Seismic vulnerability assessment of school buildings in Tehran city based on AHP and GIS. *Nat. Hazards Earth Syst. Sci.* **2014**, *14*, 969–979. [CrossRef]
5. Asef, M.R. Modeling the elements of country vulnerability to earthquake disasters. *Disasters* **2008**, *32*, 480–498. [CrossRef] [PubMed]
6. Mahdi, T.; Mahdi, A. Reconstruction and retrofitting of buildings after recent earthquakes in Iran. *Procedia Eng.* **2013**, *54*, 127–139. [CrossRef]
7. Rygel, L.; O'Sullivan, D.; Yarnal, B. A method for constructing a social vulnerability index: An application to hurricane storm surges in a developed country. *Mitig. Adapt. Strat. Glob. Chang.* **2006**, *11*, 741–764. [CrossRef]

8. Ding, H.; Ding, S.F.; Hu, L.H. Research progress of attribute reduction based on rough sets. *Comput. Eng. Sci.* **2010**, *6*, 92–94.
9. Birkmann, J. Risk and vulnerability indicators at different scales: Applicability, usefulness and policy implications. *Environ. Hazards* **2007**, *7*, 20–31. [CrossRef]
10. Wisner, B.; Blaikie, P.; Cannon, T.; Davis, I. *At Risk: Natural Hazards, People's Vulnerability and Disasters*, 2nd ed.; Routledge: Abingdon, UK, 2003; pp. 11–13.
11. Box, P.; Bird, D.; Haynes, K.; King, D. Shared responsibility and social vulnerability in the 2011 Brisbane flood. *Nat. Hazards* **2016**, *81*, 1549–1568. [CrossRef]
12. Toro, J.; Duarte, O.; Requena, I.; Zamorano, M. Determining Vulnerability Importance in Environmental Impact Assessment The case of Colombia. *Environ. Impact Assess. Rev.* **2012**, *32*, 107–117. [CrossRef]
13. Tate, E. Social vulnerability indices: A comparative assessment using uncertainty and sensitivity analysis. *Nat. Hazards* **2012**, *63*, 1–23. [CrossRef]
14. Juntunen, L. Addressing Social Vulnerability to Hazards. *Disaster Saf. Rev.* **2005**, *4*, 3–10.
15. Turner, B.L., 2nd; Kasperson, R.E.; Matson, P.A.; McCarthy, J.J.; Corell, R.W.; Christensen, L.; Eckley, N.; Kasperson, J.X.; Luers, A.; Martello, M.L.; et al. A framework for vulnerability analysis in sustainability science. *Proc. Natl. Acad. Sci. USA* **2003**, *100*, 8074–8079. [CrossRef] [PubMed]
16. Davidson, R.; Shah, H.C. A multidisciplinary urban earthquake disaster risk index. *Earth Spec.* **1997**, *13*, 211–223. [CrossRef]
17. Davidson, D.; Freudenburg, W. Gender and environmental risk concerns. *Environ. Behav.* **1996**, *28*, 302–339. [CrossRef]
18. Davidson, R.A. *An Urban Earthquake Disaster Risk Index*; The John A. Blume Earthquake Engineering Center Report No. 121; Blume Center: Stanford, CA, USA, 1997.
19. Granger, K.; Jones, T.; Leiba, M.; Scott, G. *Community Risk in Cairns: A Provisional Multi-Hazard Risk Assessment*; AGSO Cities Project Report No. 1; Australian Geological Survey Organisation: Canberra, Australia, 1999.
20. Adger, W.N.; Brooks, N.; Bentham, G.; Agnew, M.; Eriksen, S. *New Indicators of Vulnerability and Adaptive Capacity*; Tyndall Centre for Climate Change Research: Norwich, UK, 2004.
21. Cutter, S.L. Vulnerability to environmental hazards. *Progress Hum. Geogr.* **1996**, *20*, 529–539. [CrossRef]
22. Khan, S. Vulnerability assessments and their planning implications: A case study of the Hutt Valley, New Zealand. *Nat. Hazards* **2012**, *64*, 1587–1607. [CrossRef]
23. Tierney, K. Social Inequality: Humans and Disasters. In *On Risk and Disaster: Lessons from Hurricane Katrina*; Daniels, R.J., Keitl, D.F., Kunreuther, H., Eds.; University of Pennsylvania Press: Philadelphia, PA, USA, 2006.
24. Hosseini, A.; GHasemi, Z.; Ahadnejad, M.; Alimoradi, T. Evaluation of qualitative and quantitative indicators of social housing in the Tabriz metropolitan. *Int. J. Bus. Behav. Sci.* **2014**, *4*, 19–30.
25. Beccari, B. A comparative analysis of disaster risk, vulnerability and resilience composite indicators. *PLoS Curr.* **2016**, 8. [CrossRef] [PubMed]
26. Arias, P.A.; Villegas, J.C.; Machado, J.; Serna, A.M.; Vidal, L.M.; Vieira, C.; Cadavid, C.A.; Vieira, S.C. Reducing social vulnerability to environmental change: Building trust through social collaboration on environmental monitoring. *Weather Clim. Soc.* **2016**, *8*, 57–76. [CrossRef]
27. Armas, I.; Gavris, A. Social vulnerability assessment using spatial multi-criteria analysis (SEVI model) and the Social Vulnerability Index (SoVI model)—A case study for Bucharest, Romania. *Nat. Hazards Earth Syst. Sci.* **2013**, *13*, 1481–1499. [CrossRef]
28. Kasperson, J.; Kasperson, R. *The Social Contours of Risk: Risk Analysis, Corporations & the Globalization of Risk*; Earthscan: London, UK, 2005; pp. 1–2.
29. Birkmann, J. Indicators and Criteria for Measuring Vulnerability: Theoretical Bases and Requirements. In *Measuring Vulnerability to Natural Hazards: Towards Disaster Resilient Societies*; Birkman, J., Ed.; United Nations University Press: Tokyo, Japan, 2006; pp. 55–77.
30. Masozera, M.; Bailey, M.; Kerchner, C. Distribution of impacts of natural disasters across income groups: A case study of New Orleans. *Ecol. Econ.* **2007**, *63*, 299–306. [CrossRef]
31. Koks, E.E.; de Moel, H.; Aerts, J.C.J.H.; Bouwer, L.M. Effect of spatial adaptation measures on flood risk: Study of coastal floods in Belgium. *Reg. Environ. Chang.* **2014**, *14*, 413–425. [CrossRef]
32. Chen, W.; Cutter, S.L.; Emrich, C.T.; Shi, P. Measuring social vulnerability to natural hazards in the Yangtze River Delta region, China. *Int. J. Disaster Risk Sci.* **2013**, *4*, 169–181. [CrossRef]

33. Clark, G.E.; Moser, S.; Ratick, S.J.; Dow, K.; Meyer, W.B.; Emani, S.; Jin, W.; Kasperson, J.X.; Kasperson, R.E.; Schwarz, H.E. Assessing the vulnerability of coastal communities to extreme storms: The case of revere, MA, USA. *Mitig. Adapt. Strat. Glob. Chang.* **1998**, *3*, 59–82. [CrossRef]
34. Bankoff, G.; Frerks, G.; Hilhorst, D. *Mapping Vulnerability*; Earthscan: London, UK, 2004.
35. Burton, I.; Kates, R.W.; White, G.F. *The Environment as Hazard. Contemporary Sociology*; Oxford University Press: Oxford, UK, 1978.
36. Flanagan, B.E.; Gregory, E.W.; Hallisey, E.J.; Heitgerd, J.L.; Lewis, B. A social vulnerability index for disaster management. *J. Homel. Secur. Emerg. Manag.* **2011**, *8*, 33–42. [CrossRef]
37. Collins, T.W.; Grineski, S.E.; Aguilar, M.L.R. Vulnerability to environmental hazards in the Ciudad Jua'rez (Mexico)–El Paso (USA) metropolis: A model for spatial risk assessment in transnational context. *Appl. Geogr.* **2009**, *29*, 448–461. [CrossRef]
38. Cutter, S.L.; Mitchell, J.T.; Scott, M.S. Revealing the vulnerability of people and places: A case study of Georgetown County, South Carolina. *Ann. Assoc. Am. Geogr.* **2000**, *90*, 713–737. [CrossRef]
39. Wood, N.J.; Burton, C.G.; Cutter, S.L. Community variations in social vulnerability to Cascadia-related tsunamis in the U.S. Pacific Northwest. *Nat. Hazards* **2010**, *52*, 369–389. [CrossRef]
40. Cutter, S.L.; Bornuff, B.J.; Shirley, W.L. Social vulnerability to environmental hazards. *Soc. Sci. Q.* **2003**, *84*, 242–261. [CrossRef]
41. Bjarnadottir, S.; Li, Y.; Stewart, M.G. Social vulnerability index for coastal communities at risk to hurricane hazard and a changing climate. *Nat. Hazards* **2011**. [CrossRef]
42. Zhang, W.; Xu, X.; Chen, X. Social vulnerability assessment of earthquake disaster based on the catastrophe progression method: A Sichuan Province case study. *Int. J. Disaster Risk Reduct.* **2017**, *24*, 361–372. [CrossRef]
43. Thiri, M.A. Social vulnerability and environmental migration: The case of Miyagi Prefecture after the Great East Japan Earthquake. *Int. J. Disaster Risk Reduct.* **2017**, *25*, 212–226. [CrossRef]
44. Cerchiello, V.; Ceresa, P.; Monteiro, R.; Komendantova, N. Assessment of social vulnerability to seismic hazard in Nablus, Palestine. *Int. J. Disaster Risk Reduct.* **2018**, *28*, 491–506. [CrossRef]
45. JICA (Japan International Cooperation Agency) and CEST (Center for Earthquake and Environmental Studies of Tehran, Tehran Municipality). *The Study on Seismic Micro Zoning of the Greater Tehran Area in the Islamic Republic of Iran*; Final Report; Center for Earthquake and Environmental Studies of Tehran, Tehran Municipality: Tehran, Iran, 2000; p. 403.
46. Bahrainy, H. Natural Disaster Management in Iran during the 1990s—Need for a New Structure. *J. Urban Plan. Dev.* **2003**, *129*, 140–160. [CrossRef]
47. Shakib, H.; Dardaei, J.S.; Pirizadeh, M. Proposed seismic risk reduction program for the megacity of Tehran, Iran. *Nat. Hazards Rev.* **2011**, *12*, 140–145. [CrossRef]
48. Ferretti, V.; Montibeller, G. Key challenges and meta-choices in designing and applying multi-criteria spatial decision support systems. *Decis. Support Syst.* **2016**, *84*, 41–52. [CrossRef]
49. Hinton, G.E. How neural networks learn from experience. *Sci. Am.* **1992**, *267*, 145–151. [CrossRef]
50. Jensen, B. Expert Systems-Neural Networks. In *strument Engineers' Handbook*, 3rd ed.; Chilton: Radnor, PA, USA, 1994.
51. Pradhan, B.; Pirasteh, S. Comparison between prediction capabilities of neural network and fuzzy logic techniques for landslide susceptibility mapping. *Disaster Adv.* **2010**, *3*, 26–34.
52. Bishop, C.M. *Neural Networks for Pattern Recognition*; Clarendon Press: Oxford, UK, 1995.
53. Haykin, S. *Neural Networks: A Comprehensive Foundation*, 2nd ed.; Prentice Hall: Upper Saddle River, NJ, USA, 1999.
54. Hizbaron, D.R.; Baiquni, M.; Sartohadi, J.; Rijanta, R. Urban Vulnerability in Bantul District, Indonesia—Towards Safer and Sustainable Development. *Sustainability* **2012**, *4*, 2022–2037. [CrossRef]
55. Lee, S.; Ryu, J.H.; Won, J.S.; Park, H.J. Determination and application of the weights for landslide susceptibility mapping using an artificial neural network. *Eng. Geol.* **2003**, *71*, 289–302. [CrossRef]
56. Lee, S.; Choi, J.; Min, K. Probabilistic landslide hazard mapping using GIS and remote sensing data at Boun Korea. *Int. J. Remote Sens.* **2004**, *25*, 2037–2052. [CrossRef]
57. Iranian Statistics Center. *Iranian Statistical Calender*; Iranian Statistics Center: Tehran, Iran, 2011.
58. Ahour, I. The qualities of Tabriz historical bazaar in urban planning and the integration of its potentials into megamalls. *J. Geogr. Reg. Plan.* **2011**, *4*, 199–215.

59. Hessami, K.H.; Jamali, F.; Tabassi, H. *Major Active Faults of Iran*; International Institute of Earthquake Engineering and Seismology: Tehran, Iran, 2003.
60. Tavakoli, B. Sensitivity of seismic hazard evaluations to uncertainties determined from seismic source characterization. *J. Seismol.* **2002**, *6*, 525–545. [CrossRef]
61. Jackson, J. Partitioning of strike-slip and convergent motion between Eurasia and Arabiain Eastern Turkey and the Caucasus. *Geophys. Res.* **1992**, *97*, 12471–12479. [CrossRef]
62. Berberian, M. *Contribution to the Seism Tectonics of Iran (Part 2)*; Geological Survey of Iran: Tehran, Iran, 1976.
63. Berberian, M. Natural hazard sand the first earthquake catalogue of Iran. *Int. Inst. Earthq. Eng. Seismol.* **1994**, *1*, 266–270.
64. Karimzadeh, S.; Cakir, Z.; Osmanoglu, B.; Schmalzle, G.; Miyajima, M.; Amiraslanzadeh, R.; Djamour, Y. Interseismic strain accumulation across the North Tabriz Fault (NW Iran) deduced from InSAR time series. *J. Geodyn.* **2013**, *66*, 53–58. [CrossRef]
65. Ghayamghamian, M.R.; Rajool, A. Long-period Ground Motion Simulation for NTF Fault Near-source energy released. In Proceedings of the Fifteenth World Conference on Earthquake Engineering, Lisbon, Portugal, 24–28 September 2012.
66. Kenya Projects Organization. Available online: http://www.kenpro.org/sample-size-determination-using-krejcie-and-morgantable (accessed on 15 October 2014).
67. Ministry of Human Resource Development. Report of All India Survey on Higher Education (AISHE). Available online: http://aishe.nic.in/aishe/viewDocument.action?documentId=199 (accessed on 18 August 2018).
68. Krosnick, J.A. Survey research. *Annu. Rev. Psychol.* **1999**, *50*, 537–567. [CrossRef] [PubMed]
69. Kometa, S.; Olomolaiye, P. Validation of the model for evaluating client-generated risk by project consultants. *Construct. Manag. Econ.* **1997**, *14*, 131–145. [CrossRef]
70. Shash, A. Factors considered in tendering decisions by top UK contractors. *Construct. Manag. Econ.* **1993**, *11*, 111–118. [CrossRef]
71. Environmental Systems Research Institute (ESRI). *Arc GIS Network Analyst Routing, Closest Facility, and Service Area Analysis*; ESRI: Redlands, CA, USA, 2005.
72. Lek, S.; Delacoste, M.; Baran, P.; Dimopoulos, I.; Lauga, J.; Aulanier, S. Application of neural networks to modelling non-linear relationships in ecology. *Ecol. Model.* **1996**, *90*, 39–52. [CrossRef]
73. Lek, S.; Gue'gan, J.F. Artificial neural networks as a tool in ecological modelling, an introduction. *Ecol. Model.* **1999**, *120*, 65–73. [CrossRef]
74. Mas, J.F. Mapping land use/cover in a tropical coastal area using satellite sensor data, GIS and artificial neural networks. *Estuar. Coast. Shelf Sci.* **2004**, *59*, 219–230. [CrossRef]
75. Pradhan, B.; Buchroithner, M.F. Comparison and validation of landslide susceptibility maps using an artificial neural network model for three test areas in Malaysia. *Environ. Eng. Geosci.* **2010**, *16*, 107–126. [CrossRef]
76. Pradhan, B.; Lee, S. Landslide risk analysis using artificial neural network model focusing on different training sites. *Int. J. Phys. Sci.* **2009**, *3*, 1–15.
77. Paola, J.D.; Schowengerdt, R.A. Review and analysis of back propagation neural networks for classification of remotely sensed multi-spectral imagery. *Int. J. Remote Sens.* **1995**, *16*, 3033–3058. [CrossRef]
78. Nedic, V.; Despotovic, D.; Cvetanovic, S.; Despotovic, M.; Babic, S. Comparison of classical statistical methods and artificial neural network in traffic noise prediction. *Environ. Impact Assess. Rev.* **2014**, *49*, 24–30. [CrossRef]
79. Moody, J.E.; Hanson, S.J.; Lippmann, R.P. The effective number of parameters: An analysis of generalization and regularization in nonlinear learning systems. *Adv. Neural Inf. Process Syst.* **1992**, *4*, 847–854.
80. Tetko, I.V.; Livingstone, D.J.; Luik, A.I. Neural network studies. 1. Comparison of overfitting and overtraining. *J. Chem. Inf. Comput. Sci.* **1995**, *35*, 826–833. [CrossRef]
81. Santi, E.; Paloscia, S.; Pettinato, S.; Notarnicola, C.; Pasolli, L.; Pistocchi, A. Comparison between SAR soil moisture estimates and hydrological model simulations over the Scrivia test site. *Remote Sens.* **2015**, *5*, 4961–4976. [CrossRef]
82. Gomes, G.S.; Ludermir, T.B. Lima LMMR. Comparison of new activation functions in neural network for forecasting financial time series. *Neural Comput. Appl.* **2010**, *20*, 417–439. [CrossRef]
83. Karlik, B.; Olgac, A.V. Performance analysis of various activation functions in generalized MLP architectures of neural networks. *Int. J. Artif. Intell. Expert Syst.* **2011**, *1*, 111–122.

84. Abraham, A. Artificial neural networks. In *Handbook of Measuring System Design*; Wiley: New York, NY, USA, 2005.
85. UNISDR. Hyogo Framework for Action 2005–2015: Building the Resilience of Nations and Communities to Disasters, Geneva. 2007. Available online: https://www.unisdr.org/we/inform/publications/1037 (accessed on 10 July 2017).
86. Levin, S.A. Ecosystems and the biosphere as complex adaptive systems. *Ecosystems* **1998**, *1*, 431–436. [CrossRef]
87. Burton, I.; Kates, R.W.; White, G.F. *The Environment as Hazard*, 2nd ed.; Guildford: New York, NY, USA, 1993.
88. Anderson, M.B. Vulnerability. In *Disaster Prevention for Sustainable Development: Economic and Policy Issue*; Munasinghe, M., Clarke, C., Eds.; The International Decade for Natural Disaster Reduction (IDNDR) and TheWorld Bank: Washington, DC, USA, 1995; pp. 41–60.
89. UNISDR. Disaster Risk Reduction Tools and Methods for Climate Change Adaptation. 2004. Available online: http://www.unisdr.org/files/5654_DRRtoolsCCAUNFCC.pdf (accessed on 10 July 2017).
90. Jahangiri, K.; Izadkhah, Y.O.; Jamaledin Tabibi, S. A comparative study on community-based disaster management in selected countries and designing a model for Iran. *Disaster Prev. Manag. Int. J.* **2011**, *20*, 82–94. [CrossRef]